

## Intrinsic Channeling of Vortices along the $ab$ Plane in Vicinal $\text{YBa}_2\text{Cu}_3\text{O}_{7-\delta}$ Films

P. Berghuis, E. Di Bartolomeo, G. A. Wagner, and J. E. Evetts

*Department of Materials Science and Metallurgy and IRC in Superconductivity,  
Pembroke Street, Cambridge CB2 3QZ, United Kingdom*

(Received 4 April 1997)

We have measured the critical current density  $j_c$  as a function of the orientation of a magnetic field in vicinal  $\text{YBa}_2\text{Cu}_3\text{O}_{7-\delta}$  films. When both field and Lorentz force lie within the  $ab$  plane, we observe a minimum in  $j_c$ . At high temperatures, as the  $c$ -axis coherence length approaches the  $ab$ -plane distance, the minimum in  $j_c$  could not be observed, indicating that this effect is related to the breakdown of the rectilinear vortex state for fields at a small angle to the  $ab$  planes. Our results are the first demonstration of intrinsic channeling of vortex strings along the  $ab$  planes. [S0031-9007(97)04039-8]

PACS numbers: 74.60.Ge, 74.25.Ha, 74.72.Bk, 74.76.Bz

The profound effect of the planar nature of the superconducting state on the vortex structure and the vortex pinning characteristics in high- $T_c$  superconductors has been probed in many experiments. In a recent review Blatter *et al.* [1] discuss the complex vortex structures in these materials in an external field  $\mathbf{H}$  at a reduced temperature  $t = T/T_c$ . The nature of the vortex state depends on (i) the anisotropy parameter  $\varepsilon$ , (ii) the ratio  $d/\xi_{ab}(t)$  where  $d$  is the distance between the superconducting planes and  $\xi_{ab}$  the Ginzburg-Landau (GL) coherence length in the  $ab$  plane, and (iii) the angle  $\vartheta$  between the  $ab$  planes and  $\mathbf{B}$  the magnetic flux density. At sufficiently low temperatures, for angles  $|\vartheta| < \vartheta_1$  with  $\tan(\vartheta_1) = d/\xi_{ab}$ , the rectilinear vortex state breaks down and a kinked vortex structure emerges, which is fully developed for  $|\vartheta| < \vartheta_2$ , with  $\tan(\vartheta_2) = \varepsilon$ . The kinked vortex state is expected to cross over into a "locked" vortex state in which  $\mathbf{B}$  is strictly parallel to the  $ab$  planes [2], i.e.,  $\vartheta = 0$  independent of the angle  $\vartheta_H$  between  $\mathbf{H}$  and the  $ab$  planes if  $|\vartheta_H| < \vartheta_L$  the lock-in angle. At high temperatures  $T > T_{cr}$ , with  $T_{cr}$  such that the GL coherence length in the  $c$  direction  $\xi_c(T_{cr}) = \varepsilon\xi_{ab}(T_{cr}) = d/\sqrt{2}$ , a rectilinear vortex state persists for all  $\vartheta$  [3], and no lock-in transition is expected. The kinked vortex structure consists of vortex segments threading through the  $ab$  planes (pancake vortices) and vortex segments parallel to the  $ab$  planes (vortex strings). The pancake vortices have a fully developed normal core with spatial extent  $\xi_{ab}$ . In contrast, the vortex strings are characterized by a weak suppression of the order parameter  $\psi$  in the superconducting plane and a phase core which has dimensions  $d$  in the  $c$  direction and  $\Lambda = d/\varepsilon$  perpendicular to the  $c$  direction. In the case of  $\text{YBa}_2\text{Cu}_3\text{O}_7$  (YBCO) we have  $\varepsilon \sim 0.2$  [4–7],  $d \sim 1.2$  nm [8], and  $\xi_{ab}(0) \sim 1.6$  nm [5]. Thus,  $\vartheta_1 \sim 35^\circ$  and  $\vartheta_2 \sim 11^\circ$  for  $t = 0$ , and using  $\xi_c(t) \sim 0.25(1-t)^{-0.5}$  nm [5] close to the critical temperature  $T_c (= 90$  K), we have  $T_{cr} \sim 80$  K.

The kinked vortex structure significantly affects the dependence of the critical current density  $j_c(\vartheta_H)$  on the orientation of  $\mathbf{H}$ . The geometry of the vortex state gives

rise to three *bulk* pinning contributions. (In addition, surface pinning effects associated with the energy barrier for vortex penetration of the sample [9–11] may occur.) The first contribution is generally referred to as intrinsic pinning [12]. It operates in the presence of a current density  $\mathbf{j}$  such that the Lorentz force  $\mathbf{F}_L = \mathbf{j} \wedge \mathbf{B}$  on the strings acts in the  $c$  direction [13]. The second mechanism originates from the interaction between the pancake vortices and (extrinsic) defects. Because of the suppression of the order parameter over a length scale  $\xi_{ab}$ , pancake vortices interact strongly with sample defects on the scale of a few nanometers such as, e.g., oxygen vacancies or columnar defects introduced by heavy ion irradiation [14]. A third pinning contribution arises from a corresponding defect pinning of vortex strings, which occurs when the vortex strings experience a finite Lorentz force along the  $ab$  plane. Because of the small reduction of the order parameter in the superconducting planes adjacent to the string, it is expected that defect pinning of strings is much weaker than defect pinning of pancake vortices [1]. The strength of each individual pinning contribution can be probed experimentally in transport  $j_c$  measurements on samples using specific field-sample orientations. With  $\mathbf{e}_c$  a unit vector in the  $c$  direction, we define  $j_{c,\text{in}} \equiv j_c(\mathbf{B} \perp \mathbf{e}_c, \mathbf{F}_L \parallel \mathbf{e}_c)$ , associated with intrinsic pinning,  $j_{c,\text{str}} \equiv j_c(\mathbf{B} \perp \mathbf{e}_c, \mathbf{F}_L \perp \mathbf{e}_c)$ , associated with defect pinning of strings, and  $j_{c,\text{pc}} \equiv j_c(\mathbf{B} \parallel \mathbf{e}_c, \mathbf{F}_L \perp \mathbf{e}_c)$ , with pancake pinning.

An elegant way to elucidate these different pinning contributions is to measure  $j_c$  in vicinal YBCO films in which  $\mathbf{e}_c$  is rotated over an angle  $\theta_c$ , the vicinal angle, with respect to  $\mathbf{n}$ , a unit vector perpendicular to the film. For convenience we also define two vectors in the plane of the film,  $\mathbf{n}_1 = \mathbf{e}_c \wedge \mathbf{n}$  (along the  $ab$  planes) and  $\mathbf{n}_2 = \mathbf{n} \wedge (\mathbf{e}_c \wedge \mathbf{n})$  perpendicular to  $\mathbf{n}_1$ . The merits of vicinal films for the assessment of the pinning contributions in high- $T_c$  superconductors are as follows:

(i) The three critical currents  $j_{c,\text{in}}$ ,  $j_{c,\text{str}}$ , and  $j_{c,\text{pc}}$  can be measured on a *single* film in which two perpendicular tracks are patterned with directions  $\mathbf{n}_1$  and  $\mathbf{n}_2$ . In  $c$ -axis

films with the principle crystallographic axes aligned with the sample boundaries, the force free configuration  $\mathbf{j} \parallel \mathbf{H}$  inhibits the determination of  $j_{c,\text{str}}$ .

(ii) Because of the angle  $\theta_c$  between the surface and the  $c$  axis, the surface pinning contribution can be separated from bulk pinning effects in angular  $j_c$  measurements. In a recent paper we resolved bulk intrinsic pinning from surface pinning [11] in tracks with direction  $\mathbf{n}_1$ .

(iii) High quality films with  $j_c$  values comparable to  $c$ -axis films can be produced. Hence, the transport characteristics are not limited by weak link grain boundaries.

These unique features of vicinal films enable angular measurements of  $j_c$  to resolve for the first time the interconnected contributions of the Lorentz force, anisotropy, surface barrier, defect, and vortex structure to the critical current in YBCO films. In this paper we focus on the nature of defect pinning of the string segments.

Vicinal YBCO films were grown by high pressure dc sputtering [15] using a novel radiative heater design [16]. The films, with thickness  $D = 100$  nm, were deposited on a standard (001) SrTiO<sub>3</sub> substrate (sample Y0) and three vicinal SrTiO<sub>3</sub> substrates, which had a misorientation of 2° (sample Y2), 4° (Y4), and 6° (Y6) between the [100] axis and the surface. ( $\mathbf{n}_1 \parallel [010]$ ). X-ray diffraction rocking curve measurements on Y4 and Y6 confirmed vicinal YBCO growth. The (005) peak rocking curve width was 0.4°, for both Y4 and Y6. The vicinality of sample Y4 and Y6 was also confirmed by means of AFM/STM characterization of the surface topology. Detailed STM data on sample Y4 showed a regular terraced structure [11,17,18] with terrace step height  $\sim 1.2$  nm instead of the spiral-island morphology associated with  $c$ -axis growth [19,20].

After deposition Ag/Au contacts were evaporated and annealed in pure O<sub>2</sub>. Ion milling was used to pattern narrow tracks ( $11 \times 500 \mu\text{m}^2$ ) with current and voltage contacts in the standard four point geometry. Low temperature resistance and  $I$ - $V$  measurements were performed in a commercial (Oxford Instruments) flow cryostat equipped with an 8 T superconducting magnet and a sample holder with a two-axis rotation stage [21]. The temperature stability is better than 10 mK and the angular resolution is better than 0.1°. A  $1 \mu\text{V}$  criterion was used to determine  $j_c$  values. The  $T_c(R = 0)$  of the samples was 89.5 K. Because of the vicinality of the films,  $j_c$  is not isotropic in the plane of the film. For example, for Y6 at  $T = 77$  K,  $B = 0$  T, we obtained for a track aligned with the  $ab$  planes  $j_c(\mathbf{j} \parallel \mathbf{n}_1) = 4.2 \times 10^6$  A/cm<sup>2</sup>, comparable to  $c$ -axis film results. For a track along  $\mathbf{n}_2$  we obtained  $j_c = 1.6 \times 10^6$  A/cm<sup>2</sup>.

In Fig. 1 a schematic is given of the geometry used for the angular  $j_c$  measurements in an external field  $\mathbf{H}$ . The angle between  $\mathbf{H}$  and the  $ab$  plane is  $\vartheta_H$ . In our geometry the Lorentz force is always directed along the  $ab$  planes. If we assume  $\mathbf{B} \parallel \mathbf{H}$  for  $\vartheta_H = 90^\circ$  and  $\vartheta_H = 0^\circ$ , we can determine  $j_{c,\text{pc}}$  and  $j_{c,\text{str}}$  in the appropriate low temperature regime for  $\mathbf{H} \parallel \mathbf{e}_c$  and  $\mathbf{H} \perp \mathbf{e}_c$ , respectively.

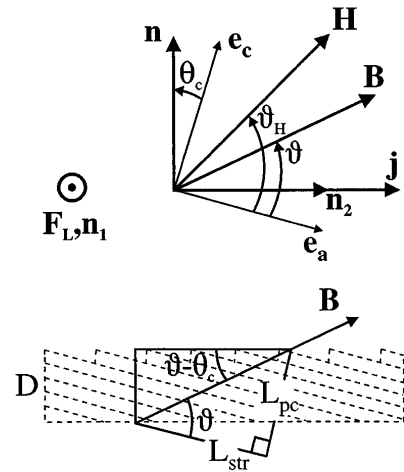


FIG. 1. Experimental geometry for the critical current measurements in vicinal YBCO films with thickness  $D$ . The current  $\mathbf{j}$  is directed along  $\mathbf{n}_2$ , a vector given by  $\mathbf{n}_2 = \mathbf{n} \wedge (\mathbf{e}_c \wedge \mathbf{n})$ , where  $\mathbf{e}_c$  and  $\mathbf{n}$  are unit vectors along the  $c$  direction and perpendicular to the plane of the film, respectively. Because of the external field  $\mathbf{H}$ , with orientation  $\vartheta_H$  penetrates the film. For  $\vartheta < \vartheta_1$  kinked vortex lines develop which are composed of pancake and string segments. The Lorentz force  $\mathbf{F}_L$  is directed along the  $ab$  planes,  $\mathbf{F}_L \parallel \mathbf{n}_1 = \mathbf{e}_c \wedge \mathbf{n}$ . The force free configuration occurs when  $\mathbf{H}$  is aligned with  $\mathbf{j}$ . The angle  $\theta_c$  between  $\mathbf{j}$  and  $\mathbf{e}_a$ , a unit vector along the  $ab$  planes perpendicular to  $\mathbf{n}_1$ , enables the determination of  $j_{c,\text{pc}}$  for  $\mathbf{H} \parallel \mathbf{e}_c$  and  $j_{c,\text{str}}$  for  $\mathbf{H} \parallel \mathbf{e}_a$ . The total length of the pancake segments  $L_{\text{pc}} [=D/\cos(\theta_c) \sim 100$  nm for  $\vartheta = 90^\circ]$  and string segments  $L_{\text{str}} [=D/\sin(\theta_c) \sim 960$  nm for  $\vartheta = 0^\circ]$  are indicated.

Therefore, this geometry is very suitable for assessing defect pinning by string segments and the relative strength of string pinning and pancake pinning. In Fig. 2 we present our main experimental result in the form of  $j_c(\vartheta_H)$  data obtained at  $\mu_0 H = 1$  T with  $T = 25$  K [Fig. 2(a)] and  $T = 76$  K [Fig. 2(b)]. For both the high and low temperature  $j_c(\vartheta_H)$  data we observe a maximum for  $\vartheta = -\theta_c$  associated with the “force free” configuration  $\mathbf{j} \parallel \mathbf{H}$ . This  $j_c$  maximum has been observed frequently in type-II superconductors and is a well known characteristic of angular  $j_c$  data. The novel feature of the low temperature  $j_c(\vartheta_H)$  data of vicinal films is the local minimum in  $j_c$  for fields aligned parallel with the  $ab$  planes ( $\vartheta_H \sim 0$ ). In contrast, at high temperatures  $T = 76$  K we do not observe a notable feature for  $\vartheta_H \sim 0$  in the  $j_c(\vartheta_H)$  data. Only in the  $dj_c/d\vartheta_H$  curve, given in the inset of Fig. 2(b), a slight asymmetry can be observed.

To further evaluate the shape of the  $j_c(\vartheta_H)$  data, we determined normalized  $j_c(\vartheta_H)/j_c(\vartheta_H = -90^\circ)$  curves for  $T = 25, 40, 60,$  and  $76$  K. These are given in Fig. 3, where we defined  $n_{j_c}(\vartheta_H) \equiv j_c(\vartheta_H)/j_c(\vartheta_H = -90^\circ)$  for convenience. It can be seen that the shape of the  $n_{j_c}(\vartheta_H)$  curves is remarkably independent of temperature for  $\vartheta_H$  values away from the  $j_c$  minimum. In the angular regime where the kinked vortex state appears ( $\vartheta_2 < |\vartheta| < \vartheta_1$ ) the scaling of the  $j_c$  curves gradually breaks down and

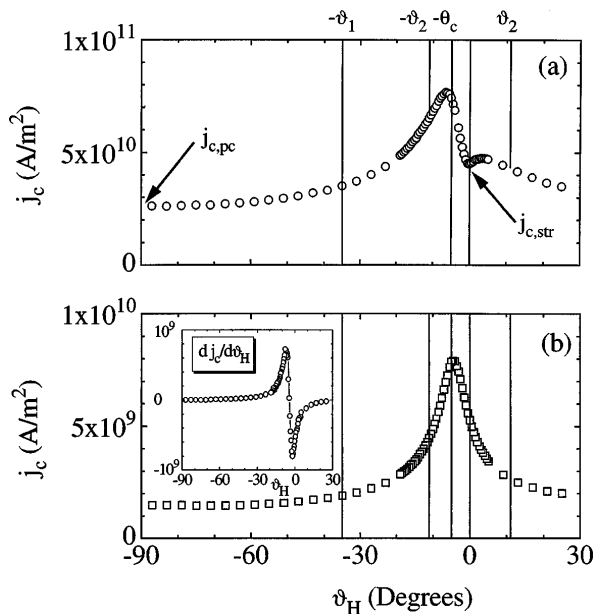


FIG. 2. Dependence of  $j_c$  on the field-sample angle  $\vartheta_H$  of sample Y6 obtained at  $\mu_0 H = 1$  T ( $10^4$  Oe). The direction of (i) the  $ab$  planes ( $\vartheta = 0$ ), (ii) the current ( $\vartheta = -\theta_c$ ), and (iii) the zero temperature values for the crossover angles  $-\vartheta_1$  and  $\pm\vartheta_2$  are denoted by vertical solid lines. The  $j_c(\vartheta_H)$  data given in (a) were taken at  $T = 25$  K ( $\circ$ ). Arrows indicate the  $j_{c,str}$  and  $j_{c,pc}$  values. In (b),  $j_c(\vartheta_H)$  data obtained at 76 K are given ( $\square$ ). The corresponding  $dj_c(\vartheta_H)/d\vartheta_H$  curve, computed numerically from the  $j_c(\vartheta_H)$  data, is given in the inset of (b). The extreme values of  $dj_c(\vartheta_H)/d\vartheta_H$  are  $7.2 \times 10^8$  and  $-8 \times 10^8$  A/m $^2$ .

for  $|\vartheta| < \vartheta_2$  the  $n_{j_c}(\vartheta_H)$  curves differ significantly. At intermediate temperatures,  $T = 40$  and 60 K, we detect a kink in  $j_c(\vartheta_H \sim 0)$  data, which develops into the  $j_c$  minimum at lower temperatures,  $T = 25$  K.

Although we cannot preclude finite pinning effects arising from  $ab$ -twin boundaries (TB) and surface steps, we would argue that these extrinsic structural features cannot account for the  $j_c$  minimum. The anisotropic pinning

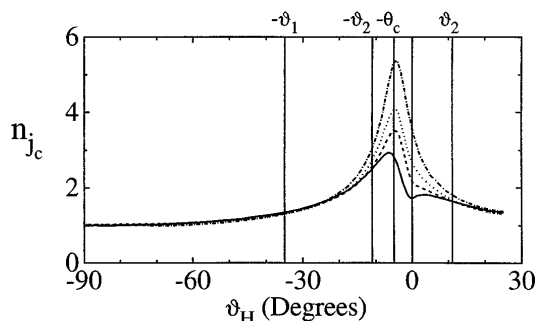


FIG. 3. Dependence of  $n_{j_c}$  on  $\vartheta_H$  for sample, Y6, obtained at  $\mu_0 H = 1$  T at temperatures  $T = 25$  K (—), 40 K (---), 60 K (···), and  $T = 76$  K (-·-·). The  $j_c(\vartheta_H = -90^\circ)$  data used to obtain  $n_{j_c}(\vartheta_H)$  are  $2.6 \times 10^{10}$  A/m $^2$  (25 K),  $1.6 \times 10^{10}$  A/m $^2$  (40 K),  $6.25 \times 10^9$  A/m $^2$  (60 K), and  $1.47 \times 10^9$  A/m $^2$  (76 K). Solid vertical lines denote the direction of the  $ab$  planes, the current,  $\vartheta_1$ , and  $\vartheta_2$ .

characteristics of TB planes ( $\perp$  to the  $ab$  plane) do not provide a probable explanation since we cannot invoke a sharp change in the angle between the TB and both  $\mathbf{H}$  and  $\mathbf{F}_L$  around the  $j_c$  minimum in our experiment. We expect pinning of pancakes at the surface steps to be rather weak in our geometry since vortex motion occurs along the surface steps ( $\mathbf{F}_L \parallel \mathbf{n}_1$ ). Furthermore, preliminary measurements by us in a different geometry of the vortex structure with respect to the surface steps with  $\mathbf{j} \parallel \mathbf{n}_2$  and  $\mathbf{n}_2$  rotation axis of  $\mathbf{H}$  show a similar  $j_c$  minimum for  $\mathbf{H} \parallel \mathbf{n}_1$ , i.e.,  $\mathbf{F}_L \parallel \mathbf{n}$ . This result supports the view that the  $j_c$  minimum is a bulk effect. The appearance of the  $j_c$  anomaly in the presence of a finite component of  $\mathbf{F}_L$  along the  $ab$  plane for  $|\vartheta| < \vartheta_1$  and  $T < T_{cr}$  suggests an intrinsic origin related to the development of the kinked vortex state. In this scenario the  $j_c$  minimum arises from the weak interaction between vortex strings and extrinsic defects, providing a channel along  $ab$  planes characterized by a significantly reduced macroscopic pinning force density  $\mathbf{F}_p = \mathbf{j} \wedge \mathbf{B}$ . Since the Lorentz force does not depend on the anisotropy but depends on macroscopic field equations, we can assess the relative strength of the pinning force per unit length of vortex strings  $f_{p,str}$  and pancakes  $f_{p,pc}$  from the  $j_{c,pc}$  and  $j_{c,str}$  data. From the force balance equation for a vortex string,  $f_L = f_{p,str} L_{str}$ , where  $f_L = j_{c,str} \phi_0 D$  represents the total Lorentz force acting on the vortex string and  $L_{str} = D/\sin(\theta_c)$  the length of the vortex string, we obtain  $f_{p,str} = j_{c,str} \phi_0 \sin(\theta_c)$  for  $\vartheta_H = 0$ . Following an analogous consideration for the pinning of a vortex line consisting of pancake segments we obtain  $f_{p,pc} = j_{c,pc} \phi_0 \cos(\theta_c)$ . The ratio  $R_p \equiv f_{p,str}/f_{p,pc}$  can now be expressed in terms of  $n_{j_c}(\vartheta_H)$  as

$$R_p = n_{j_c}(0) \tan(\theta_c). \quad (1)$$

In Fig. 4 we present the  $T$  dependence of the  $R_p$  data according to Eq. (1) for fields ranging from 1 to 6 T. It can be seen that the dependence of  $R_p$  on  $H$  is weak. Both  $j_{c,pc}$  and  $j_{c,str}$  do depend on  $H$ , which can be related to either collective effects or a distribution in the strength of the pinning centers. The weak  $H$  dependence of  $R_p$  suggests that the defects responsible for pinning and the pinning regime are similar for both vortex pancakes and vortex strings. Blatter *et al.* [1] consider point defects as pinning centers for both pancakes and strings and obtain at low fields in the single vortex regime  $R_p \sim \varepsilon(\xi_{ab}/\Lambda)^3$  which becomes  $\sim 4.8 \times 10^{-3}$  at low temperatures. Our values for  $R_p$  are larger than this estimate. In Fig. 4 we give the curve  $0.68\xi_{ab}(T)/\Lambda$ , and it can be seen that the experimental  $R_p$  data follow the  $T$  dependence of  $\xi_{ab}$ . A possible explanation for the deviation between theory and experiment would be the presence of strongly pinned pancake vortices in the film even when the field is aligned with the  $ab$  planes due to (i) self-field effects ( $\sim 1$  mT) and (ii) the mosaic spread in  $c$ -axis directions ( $\sim 0.4^\circ$ ). However, to reconcile the observed  $j_{c,str}$  value at 25 K and 1 T with the estimate of Blatter would require

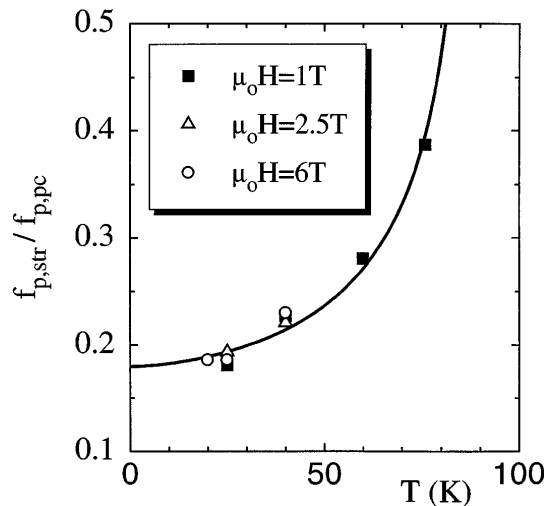


FIG. 4. Temperature dependence of  $R_p \equiv f_{p,\text{str}}/f_{p,\text{pc}}$  obtained at  $\mu_0 H = 1$  T (■), 2.5 T (△), and 6 T (○). The solid line displays  $0.68\xi_{ab}/\Lambda$ . We determined  $\xi_{ab}(T)$  using the expression  $\xi_{ab}(T) = \xi_{ab}(0)/\sqrt{f_{WH}(T)}$  with  $f_{WH}(T)$  the Werthamer function [23].

an unrealistically large perpendicular component of the field,  $\sim 40$  mT at  $\vartheta_H = 0$  [22]. Although string pinning is clearly very significant for  $j_c(\vartheta_H \sim 0)$  a quantitative analysis should take into account the presence of residual pancakes in the film by addressing the local misorientation between  $\mathbf{H}$  and  $\mathbf{B}$ .

In conclusion, we have measured for the first time the critical current density associated with defect pinning of vortex strings in vicinal YBCO films and shown that it is weaker than pinning of vortex pancakes, in accordance with the theoretical expectation [1]. Clearly pinning of vortex strings is very anisotropic resulting in the observed channeling effects for motion of vortex strings along the  $ab$  planes and very strong intrinsic pinning for perpendicular motion. This work indicates that the distinction between a kinked vortex structure at low temperatures and a rectilinear structure at high temperatures is of major importance, and we confirm that the onset of the kinked vortex state occurs close to 80 K in YBCO. Our use of vicinal films enables the usual symmetry of a transport measurement to be reduced, and this strategy could also be used to assess other transport properties such as thermopower and Hall effect in which the direction of the vortex motion plays a determining role.

We would like to acknowledge support for this work from the EPSRC and the HCM network "Flux Pinning in High- $T_c$  Superconductors" of the EC.

[1] G. Blatter *et al.*, Rev. Mod. Phys. **66**, 1125 (1994).

- [2] D. Feinberg and C. Villard, Phys. Rev. Lett. **65**, 919 (1990).
- [3] D. E. Farrell *et al.*, Phys. Rev. Lett. **64**, 1573 (1990).
- [4] D. E. Farrell *et al.*, Phys. Rev. Lett. **61**, 2805 (1988).
- [5] U. Welp *et al.*, Phys. Rev. Lett. **62**, 1908 (1989).
- [6] L. Y. Vinnikov *et al.*, J. Phys. B **49**, 99 (1989).
- [7] G. J. Dolan *et al.*, Phys. Rev. Lett. **62**, 2184 (1989).
- [8] R. J. Cava *et al.*, Phys. Rev. Lett. **58**, 1676 (1987).
- [9] C. P. Bean and J. D. Livingston, Phys. Rev. Lett. **12**, 14 (1964).
- [10] L. Burlachkov *et al.*, Phys. Rev. B **50**, 16770 (1994).
- [11] P. Berghuis *et al.*, in *Proceedings of the 8th IWCC in Superconductors, Kitakyushu, Japan, 1996*, edited by T. M. Matsushita and K. Yamafuji (World Scientific, Singapore, 1996), p. 247.
- [12] M. Tachiki, S. Takahashi, and K. Sunaga, Phys. Rev. B **47**, 6095 (1993).
- [13] R. A. Doyle, A. M. Campbell, and R. E. Somekh, Phys. Rev. Lett. **71**, 4241 (1993).
- [14] L. Civale *et al.*, Phys. Rev. Lett. **67**, 648 (1991).
- [15] R. E. Somekh and Z. H. Barber, in *Physics and Materials Science of High Temperature Superconductors II*, edited by R. Kossowsky (Kluwer, Amsterdam, 1992), p. 443.
- [16] G. A. Wagner, R. E. Somekh, and J. E. Evetts, in *Proceedings of EUCAS, Edinburgh, UK, 1995*, edited by D. Dew-Hughes (IOP, London, 1995), p. 855.
- [17] D. H. Lowndes *et al.*, Appl. Phys. Lett. **61**, 852 (1992).
- [18] T. Haage *et al.*, Solid State Commun. **99**, 553 (1996).
- [19] M. Hawley *et al.*, Science **251**, 1587 (1991).
- [20] C. Gerber *et al.*, Nature (London) **350**, 279 (1991).
- [21] R. Herzog and J. E. Evetts, Rev. Sci. Instrum. **65**, 3574 (1994).
- [22] The contribution of residual pancake vortices to the pinning characteristics at  $\vartheta_H = 0$  can be evaluated as follows. The mosaic spread  $\theta_m \sim 0.4^\circ$  gives rise to an average perpendicular field component  $B_r$  of 7 mT in an applied field  $\mu_0 H = 1$  T. In this situation a vortex line consists of string segments with total length  $L_{\text{str}} \sim D/\sin(\theta_c)$  and residual pancake segments with total length  $L_{\text{pc},r} \sim D \sin(\theta_m)/\sin(\theta_c)$ . The pinning force  $f_r$  arising from the residual pancakes on a vortex line can be estimated as  $f_r \approx f_{p,\text{pc}}(B = 7 \text{ mT})L_{\text{pc},r}$ . Using this expression, the relative contribution  $f_r/f_L$  to the force balance at  $\vartheta_H = 0$  and  $\mu_0 H = 1$  T can be written as  $f_r/f_L \approx j_{c,\text{pc}}(B = 7 \text{ mT}) \sin(\theta_m) \{j_{c,\text{str}}(B = 1 \text{ T}) \tan(\theta_c)\}^{-1}$ . At 76 K we measured  $j_{c,\text{pc}}(B = 7 \text{ mT}) = 1.55 \times 10^6 \text{ A/cm}^2$  and  $j_{c,\text{str}}(B = 1 \text{ T}) = 5.3 \times 10^5 \text{ A/cm}^2$  which implies  $f_r/f_L \sim 20\%$ . At low temperatures  $f_r/f_L$  becomes  $\sim 12\%$ . Thus, the correction would result in a reduction of  $R_p$  but would not significantly alter the observed  $B$  and  $T$  dependence of  $R_p$ . The correction required for a low temperature  $R_p$  value consistent with [1] would imply  $B_r \sim 40$  mT.
- [23] R. H. Werthamer, E. Helfand, and P. C. Hohenberg, Phys. Rev. **147**, 295 (1966).